Guangju, Xu; Yang, Zhao; Mingdi, Li; Ling, Lin; Yanbin, Hu

Article

Effects of the lubricating oil and diesel mixture combustion on the oxidation and microphysical properties of particulate matter

Energy Reports

Provided in Cooperation with:
Elsevier

Suggested Citation: Guangju, Xu; Yang, Zhao; Mingdi, Li; Ling, Lin; Yanbin, Hu (2020) : Effects of the lubricating oil and diesel mixture combustion on the oxidation and microphysical properties of particulate matter, Energy Reports, ISSN 2352-4847, Elsevier, Amsterdam, Vol. 6, pp. 308-314, https://doi.org/10.1016/j.egyr.2020.01.004

Energy Reports 6 (2020) 308–314

Contents lists available at ScienceDirect

Energy Reports

journal homepage: www.elsevier.com/locate/egyr

Research Paper

Effects of the lubricating oil and diesel mixture combustion on the oxidation and microphysical properties of particulate matter

Xu Guangju *, Zhao Yang, Li Mingdi, Lin Ling, Hu Yanbin

School of Automotive Engineering, Changshu Institute of Technology, Changshu 215500, China

ARTICLE INFO

Article history:
Received 4 February 2018
Received in revised form 6 January 2020
Accepted 13 January 2020
Available online xxxx

Keywords:
Lubricating oil
Emission characteristics
Interlayer spacing
Microcrystalline size
Tortuosity
Degree of graphitization

ABSTRACT

This research focuses on the diesel and diesel/oil mixed fuel combustion particles as the research object and analyzes the characteristics of the two kinds of fuel oil under different parameters. The characteristics of the combustion particulate matter in the DPF discharge of the two fuels before and after carrying out TEM imaging of the sample particles were studied. The TEM image was obtained, and the morphology characteristics, level spacing, crystallite size, and curvature were discussed. The microstructure characteristics of the particulate samples were determined with Raman spectroscopy to analyze the degree of graphitization of the particulate matter. The results show that, during combustion, the lubricating oil is easily cracked to produce insoluble particles, sulfate and ash. The insoluble particles tend to saturate and condense into nuclei during the exhaust and dilution processes, which leads to an increase in the modal accumulation particles. The combustion of the lubricating oil has a great influence on the working efficiency of the DPF posttreatment system.

1. Introduction

Lubricating oil is an important material to ensure the normal operation of internal combustion engines. The quality of lubricating oil is directly related to the reliability, economy and emission of the internal combustion engine (Jiao et al., 2017; Martini et al., 2018; R'Mili et al., 2018; Serrano et al., 2017; Tan et al., 2018). The combustion of lubricating oil will affect soot, ash, soluble organic components, metal elements and other pollutants, and the improvement of emission control technology for internal combustion engines has proposed higher requirements on the adaptability of lubricating oil.

To further the theoretical understanding of the lubricating oil quality, researchers around the world have conducted extensive research on the lubricating oil-derived DEPM (diesel exhaust particulate matter) emissions, soluble organic matter (OM) with PM adhering to its surface and kinetic processes of combustion chemical reactions involving lubricating oil. Sonntag et al. (2012) used the lubricating oil consumption path tracing method to study the contribution and influence mechanism of the lubricating oil for light-duty vehicle particulate emissions. Their experimental results showed that lubricating oil was responsible for approximately 25% of the weighted PM emissions from light-duty vehicles. In addition, the lubricating oil consumption tracing results showed that under partial loading, the lubricating oil contributed relatively significantly to the nanometer-scale PM emissions; when the PM size was expanded to the nanometer-scale, reducing the sulfur and additive contents of the lubricating oil would not necessarily reduce the nanometer-scale PM emissions from a diesel engine. Worton et al. (2014) used ionization gas chromatography with vacuum ultraviolet mass spectrometry to conduct the chemical characterization of organic aerosols in automobile exhaust. The results show that the main ingredients of the POA were benzene ring \naphthene (80% or higher) and n-alkanes (<5%), and the index parameters (such as carbon atomic number, double bond yields, molecular branching degree, et al.) have a higher similarity with the composition of the lubricating oil. Wei et al. (2014b) analyzed the effects of the metal elements in the lubricating oil based on the oxidative properties of the PM. They found that adding the lubricating oil to the diesel fuel at a ratio of 2% resulted in a decrease in the ignition temperature of the PM by approximately 150–200 °C, a significant increase in its oxidation rate and a slight change in its activation energy (a decrease from 108 to 101 J mol^{-1} only). Tan et al., 2018; Tan and Wang, 2017 studied the effect of sulfur content and ash content in the lubricating oil on the PM aggregation morphology and nanostructure. The results show that with the increase in sulfur content and ash content in the lubricating oil, the particles tend to change from chain structures to complex and disordered agglomeration structures, the average diameter of the primary particles increases, the length of the fringe of the primary particle nanostructures shortens, and the oxidation activity of the particles decreases. Dong et al. (2015) examined the effects of a lubricating

* Corresponding author.
E-mail address: xuguangju@cslg.edu.cn (G.J. Xu).

https://doi.org/10.1016/j.egyr.2020.01.004

oil and its additives on the PM emissions and its microproperties using the total cylinder sampling technique and found that the consumption of a small amount of the lubricating oil could still affect the particle size distribution of the emitted PM, resulting in an increase in the nucleation mode PM emissions. In addition, they also found that there was a significant difference between the effects of the additives of different types on the PM emissions and, under some conditions, the special chemical properties of the additives could even lead to a decrease in the PM emissions from the diesel engine. Moreover, they noted that the lubricating oil quality in the traditional sense was disproportionate to its effects on the PM emissions.

From the perspective of source control, fuel and lubricating oil are the two major sources of PM emissions from ICE. With the gradual upgrades i fuel quality, the lubricating oil will become the most important factor affecting the PM emissions of ICE, and the production of soluble particles, ash deposition and insoluble particles, especially sulfate, from the consumption of the lubricating oil, combustion of the additives and pyrolysis of the base oil will pose new challenges to the purification efficiency of posttreatment units; however, previous studies have paid little attention to this. Therefore, a pure diesel fuel and a pure diesel fuel/lubricating oil mixture were used as the research focus, and the experiment was carried out by a fuel quality measurement analysis. The particle samples before and after the DPF posttreatment system were collected, and the particle size distribution characteristics and microscopic physical properties were studied by using particle size spectrometry, TEM and laser Raman spectroscopy test equipment. The purpose of the current work is to gain an in-depth understanding of the particles produced by the lubricating oil combustion, including the particle size distribution rule, combustion characteristic index, interlayer spacing, microcrystalline size, tortuosity and graphitization degree. This research provides reference data for the scientific and reasonable development of DPF control strategies.

2. Experimental apparatus and methods

2.1. Test fuel

There are two kinds of fuel used in the test. One is a pure diesel that meets the five-stage fuel standard of China, and the other is a pure diesel mixed with lubricating oil (mobil 15w–40). The mixed fuel refers to the lubricating oil mixed into the diesel at 1% volume percentage. The lubricating oil with the mixed fuel is consistent with the type of lubricating oil actually used in the diesel test engine.

2.2. Test diesel engine

The experiment was conducted on a high-pressure common-rail diesel engine. The technical parameters of the diesel engine are as follows: model: JX493ZLQ3; turbocharged; four cylinder; cylinder diameter: 93 mm; piston stroke: 102 mm; displacement: 2.77 L; total power/rotational speed: 85 kW/3600 r/min; maximum torque/rotational speed: 285 N/2000 r/min; and compression ratio: 17.2. During the particle collection process, the diesel engine had a stable rotation speed of 2000 r/min and a power of 53 kW. The injection pressure was 135 MPa, the injection timing was 10° CA BTDC, and the time interval between the preinjection and main injection was 2200 μs. The diesel engine is equipped with a wall-flow DPF, the carrier material is SiC, the catalyst is the precious metal platinum Pt, the pore number is 200, and the coating content is 10 g/ft3.

2.3. Test equipment

The research equipment involved in this paper mainly includes a fuel quality analyzer, particle size spectrometer, transmission electron microscope and laser Raman spectrometer.

The fuels were tested using a MINISCAN fuel quality analyzer. The main technical specifications of the analyzer are as follows: measuring range for the cetane number: 20–80; measuring range for the total aromatic hydrocarbons: 0%–80%; measuring range for the polycyclic aromatic hydrocarbons (PAHs): 0%–50%; and measuring range for the kinematic viscosity: 0–10 m/s (40 °C). The testing was based on the partial least-squares method and an advanced chemical model that met the ASTM E1655 standard.

Particle size was analyzed via a WPS-1000XP wide range particle diameter spectrometer by MSP Corporation. The major parameters of this equipment are as follows: the sampling flow rate of 10 L/min; the particle size analysis range of 5 nm to ∼10 000 nm (0.005 ∼10 μm) and the number of particle analysis channels of 120. In the test, a particle size spectrometer was preheated for 30 min. The diesel engine dilution ratio of the exhaust versus the air was adjusted via a dilutor. After 10 min of stable diesel engine operation, data was collected, and the duration for a single data collection instance was 1 min.

An FEI TecnaiG2 F20 field-emission transmission electron microscope (TEM) was used to analyze the crystalline structure of the primary C particles (PCPs) comprising each DEPM sample. The main technical specifications of the TEM are as follows: accelerating voltage: 200 kV; magnification: 25,000–1,030,000 times; point resolution: 0.24 nm; line resolution: 0.102 nm; data resolution: 0.14 nm; angle of inclination of the sample: $<\pm 30°$; camera constant: 30–4500 mm; electronic gun: Schottky thermal field-emission electron gun; and coefficient of spherical aberration/coefficient of chromatic aberration: 1.2 mm/1.2 mm.

A HORIBA Jobin Yvon LabRAMHR800 laser confocal microscopic Raman spectrometer was used to analyze the degree of graphitization of each DEPM sample. The main specifications of the Raman spectrometer are as follows: laser wavelength: 514 nm; wavenumber accuracy: $\leq$0.1 cm^{-1}; spectral resolution: 1 cm^{-1}; Raman shift range: 50–4000 cm^{-1}; and microscopic size range: $\geq$1 μm.

2.4. Research program

The research program of the current work is as follows and shown in Fig. 1. Before the start of the experiment, pure diesel and mixed fuel were left standing for 24 h, and no stratification of the lubricating oil and diesel was found in the mixed fuel. First, we carried out a fuel quality test of the diesel and diesel/lubricating oil mixtures to obtain the physical and chemical performance indexes of the two tested fuels. The diesel engine bench test was carried out, and the particle size distribution before and after the DPF was compared and analyzed by particle size spectrometry. The particle samples before and after the DPF were collected, and the microscopic physical properties of the particles were studied by TEM and laser Raman spectrometry.

The working process of DPF is divided into four stages, ① 1 h of PM loading, ② 0.5 h of active regeneration, ③ 4.5 h of passive regeneration, ④ 0.25 h of active regeneration. Thus, an experimental cycle has been completed, and three experimental cycles have been carried out in total. The measurement of exhaust particle concentration after DPF filtration was completed at the PM loading stage, considering the pressure drop caused by DPF filter channel blockage due to PM accumulation, the test was completed within the first 10 min of the PM loading stage, and the average value of three measurements was used to evaluate the effect of DPF on the concentration of tested fuel exhaust particles.

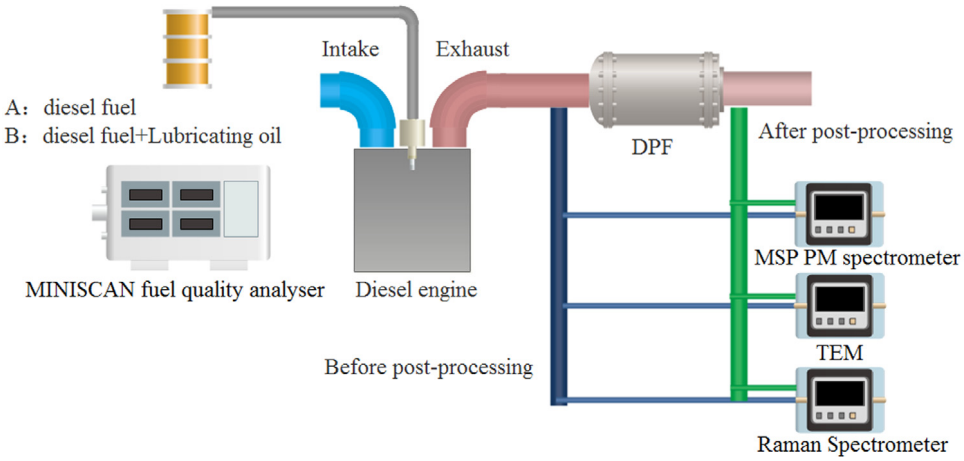

Fig. 1. Schematic diagram of the experimental setup.

3. Results and discussion

3.1. Fuel quality test results of the two test fuels

Fig. 2 shows the physical and chemical properties of the two test fuels. The data obtained in this experiment are the results obtained by averaging the six measurements. We mainly analyzed the cetane number, total aromatic hydrocarbon content, polycyclic aromatic hydrocarbon content and T90 temperature. Compared with pure diesel, the cetane number of the mixed fuel increased by 1.9, the total aromatic hydrocarbon content increased by 1.3%, the polycyclic aromatic hydrocarbon content increased by 0.8, and the fuel distillation characteristic temperature T90 increased by 6 °C.

The reason is that the lubricating oil is mainly composed of a base oil and lubricating oil additives. The main components of the base oil are alkanes, naphthenes, aromatic hydrocarbons, cycloalkyl aromatic hydrocarbons and nonhydrocarbon compounds. Commonly used lubricating oil additives include antioxidants, detergents, foam inhibitors, antiwear agents, etc., and most of these additives are long carbon chain components. For example, the antioxidant zinc dialkylphosphorodithiloate has the formula C28H60O4P2S4Zn.

The long carbon chain component in the lubricating oil increases the cetane number of the mixed fuel, and the distillation characteristic temperature T90 of the mixed fuel increases due to the increase in heavy components such as the polycyclic aromatic hydrocarbons. The change in the content of the polycyclic aromatic hydrocarbons in the fuel will also affect the particle emission and further affect the working efficiency of the DPF posttreatment system.

3.2. Results of particle size analysis

As shown in Fig. 3, the diesel fuel and diesel/lubricating oil mixed fuel were used for the bench test in this work, and the particle concentration and particle size distribution before and after the DPF were collected and analyzed under the same working conditions. The particle size of the particles produced by the two fuels is mainly distributed in the range of 0–300 nm. After the DPF posttreatment system, the concentration of the combustion particles of the two fuels is greatly reduced.

Before the DPF, when pure diesel was used, the concentration of particles showed a two-peak distribution. The peak concentration and its corresponding particle size were 5.25×10^7 (cm^3)/19 nm and 6.42×10^7 (cm^3)/107 nm, respectively. When

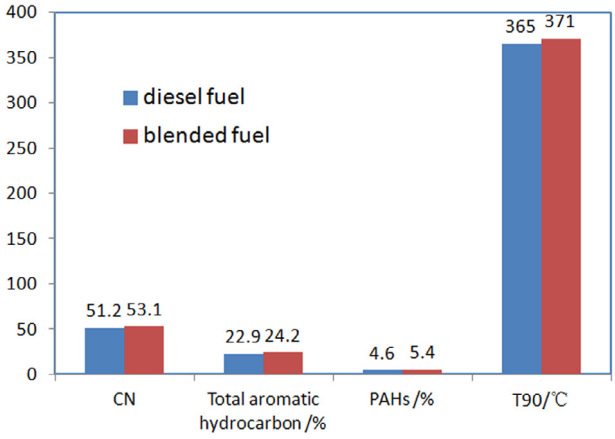

Fig. 2. Fuel quality test results of the test fuels.

the diesel/lubricating oil mixed fuel was used, the peak concentration and its corresponding particle size were 2.81×10^7 (cm^3)/20 nm and 9.46×10^7 (cm^3)/93 nm, respectively. In terms of the particle size, the particles are mainly distributed in the nuclear mode region at approximately 20 nm and the accumulation mode region at approximately 100 nm. Compared with pure diesel, the peak particle concentration in the nuclear mode decreased by 46.5%, but the peak particle concentration in the accumulated mode increased by 47.4%. The reason is that during combustion, the lubricating oil cracks to produce insoluble particles, sulfates and ash and tends to reach the saturation state and condense into nuclei during the exhaust and dilution, leading to an increase in the number of accumulated modal particles.

The distribution of exhaust particle concentration of the two test fuels after DPF filtration were measured, these particles are those that can pass through the filter channels of DPF, the results show that, particle size of the two fuels was mainly concentrated in the range of 10 nm–140 nm, and the particle concentration of pure diesel fuel was relatively flat in the range of the particle size, no longer having an obvious peak concentration, and the concentration was basically maintained at approximately 3.8×10^4 (cm^3), indicating that the DPF had a high particle collection efficiency. Burning the diesel oil/oil mixed fuel still offers a bimodal particle shape, and the average particle concentration was approximately 16.9×10^4 (cm^3), which is far higher than that of the pure diesel particulate matter, suggesting that the lubricating oil in the combustion of the DPF postprocessing system has a

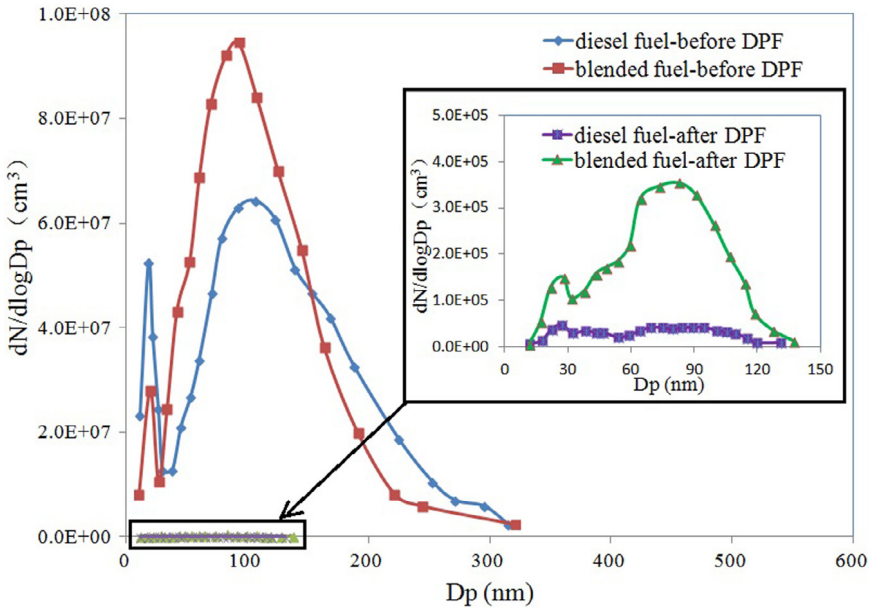

Fig. 3. Particle size distribution characteristics of the two tested fuels before and after the DPF.

great influence on the work efficiency because the oil particle emissions deserve more attention.

3.3. Microscopic physical properties of the particles

3.3.1. Appearance characteristics

Fig. 4 shows the TEM images of the combustion particles of the two test fuels with a magnification of 600,000 times. Under the action of an interparticle liquid bridge and solid bridge forces, the combustion particles of the pure diesel oil form a chain structure with a single interparticle connection and present different densification degrees at the junction. Several basic carbon particles collide and overlap, forming the darker part in the TEM image. For the diesel/lubricating oil blends, the number of the individual particles increases, the size decreases, and the particle clusters are distributed in a circular pattern (Lin et al., 2017; Bott et al., 2017). Compared to the two kinds of fuel particle morphology characteristics, the lubricating oil in the combustion has an irregular shape, and the boundary of the particles increases the soluble organic matter particle content because the oil will not burn or it has inadequate combustion, leading to a smoldering lubricant adhering to the surface of the particulate matter. The generated particles in the impact process are easier to combine, and they overlap each other.

The basic components of the particulate matter are approximately spherical basic carbon particles with extremely complex structures (Llamas et al., 2017; Zhang et al., 2017; Hou et al., 2017). Therefore, Digital Micrograph software was used in this study to select the 10 TEM images with an obvious basic contour according to the requirements of statistics, to accurately and quantitatively extract and analyze the microstructure parameters of the basic carbon particles and to explore the influence of the lubricating oil participation in the combustion on the microstructure of the carbon particles. The interlayer spacing, microcrystalline size and tortuosity of the carbon particles were analyzed. Fig. 5 is a schematic diagram of the structural characteristics of the basic carbon particles.

Tortuosity: $C = \frac{La}{Lb}$

La—Microcrystalline size (nm)
Lb—The linear distance between two pixel points (nm)
d —Interlayer spacing

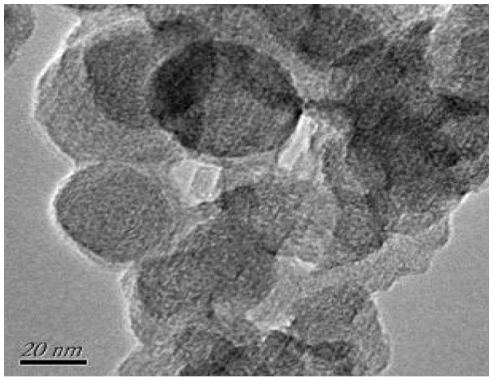

（a）Diesel fuel

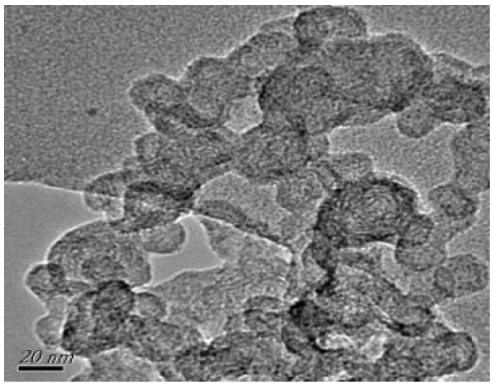

（b）Blended fuel

Fig. 4. TEM images of the particulate matter from the two test fuels.

3.3.2. Interlayer spacing

The interlayer spacing refers to the vertical distance between the two adjacent and parallel carbon layers in the basic carbon particles (Yehliu et al., 2011b,a; Hays and Vander Wal, 2007). The gray distribution of the particle graphite layer is measured in the vertical direction of the graphite layer by means of the TEM

Tortuosity: $C = \frac{La}{Lb}$

La——Microcrystalline size（nm）

Lb——The linear distance between two pixel points (nm)

d ——Interlayer spacing

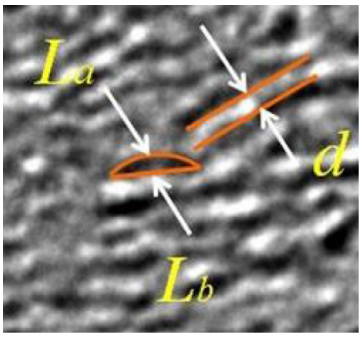

Fig. 5. A schematic diagram of the structural characteristics of the basic carbon particles.

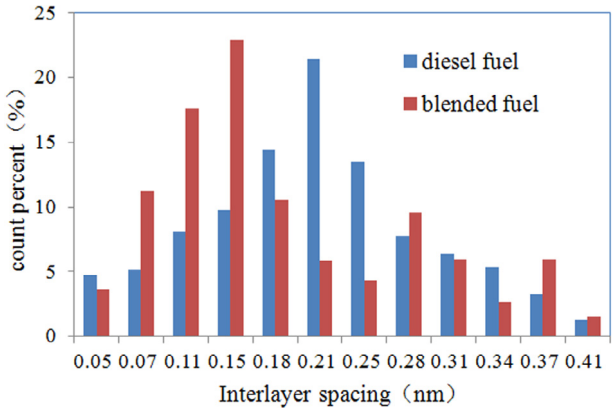

Fig. 6. Interlayer spacing of the particulate matter from the two test fuels.

image grayscale measurement. The distance between the two peaks is the interlayer spacing. To reduce the measurement error, the average of the three interlayer spacing distances is taken as the interlayer spacing of the graphite layer. The interlayer spacing reflects the oxidation activity of the formation of the basic carbon particles. The smaller the layer spacing is, the smaller the contact area of the reaction between the microcrystalline carbon layer and the oxygen will be, the oxidation difficulty will increase, and the oxidation activity will decrease.

Fig. 6 shows the calculation results of the particle spacing of the two tested fuels. According to the distribution of the basic carbon particles with the different interlayer spacings, the interlayer spacing of the pure diesel combustion is mainly between 0.18 nm and 0.25 nm, with the largest proportion being 0.21 nm. The interlayer spacing of the particulate matter in the diesel/lubricating oil mixture was mainly between 0.07 nm and 0.15 nm, with the largest proportion being 0.15 nm. The lubricating oil is involved in the combustion, which leads to the reduction in the layer spacing of the particles. From a composition viewpoint, the major components of the diesel have carbon numbers ranging between C7 ∼ C20, and the major components of the lubricating oil have carbon numbers ranging between C17 ∼ C35; the lubricating oil is easily cracked into volatile substances in the combustion process, and during the process of exhaust and dilution, it is easy

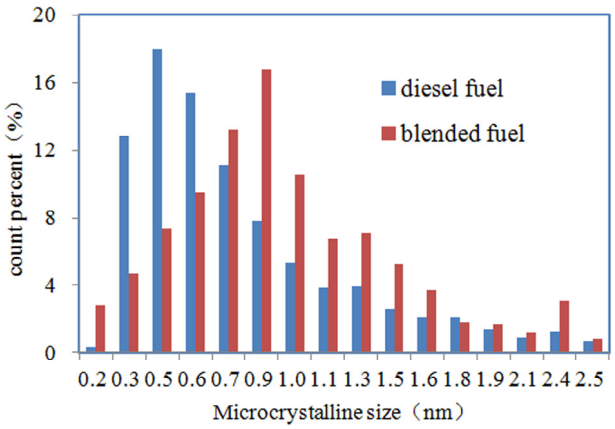

Fig. 7. Microcrystalline size of the particulate matter from the two test fuels.

to achieve the supersaturated state and then condense into the nucleated state to generate a large number of nucleated particles. In addition, the oxygen content of the lubricating oil is higher; the C and H have more opportunity to participate in the combustion process and in the oxygen reaction, prompting the particles to crack into smaller sized particles, which leads to decreased levels in particulate matter spacing and particulate matter that is not easily oxidized.

3.3.3. Microcrystalline size

The morphological and structural characteristics of the soot particles not only determine the physical morphology and aggregation degree of the soot particles but are also one of the decisive factors for their oxidation characteristics. The microcrystalline size refers to the length of a single microcrystalline carbon layer on the TEM image because carbon atoms at the edge of the carbon layer have unpaired sp2 electrons, and they are more likely to bond to oxygen (Wang, 2011; Lin et al., 2018). In other words, the smaller the size of the microcrystal, the more relative number of carbon atoms at the edge of the carbon layer, and the stronger the oxidation activity of the particles.

Fig. 7 shows the microcrystalline size calculated based on selected TEM images. The microcrystalline size of pure diesel is mainly concentrated at 0.3 nm ∼ 0.7 nm, and the proportion of the basic carbon particles with a microcrystalline size of 0.5 nm is the highest. The particle size of the blended fuel is mainly between 0.6 nm and 1.0 nm, and the proportion of the basic carbon particles with a microcrystalline size of 0.9 nm is the highest. In other words, after the combustion of the lubricating oil, due to the collision and coagulation of the ash content of the lubricating oil, the microcrystalline length of the carbon smoke particles increases, the degree of the carbon layer structure is improved, and the particles are not easily oxidized and decomposed, which is basically consistent with the conclusion obtained in Fig. 3.

3.3.4. Tortuosity

Tortuosity reflects the curvature and undulation of the carbon layer, which is related to the degree of disorder in the arrangement of carbon materials. Tortuosity is usually represented by the ratio of the length of the carbon layer to the linear distance between its endpoints. The more curved the carbon layer, the higher the value of tortuosity (Jin et al., 2014; Wei et al., 2014a). The bending of the carbon layer was caused by a 5-membered ring in the aromatic structure. Due to the overlap of the electron orbitals in the structure of the 5-membered ring, the stability of the electron resonance decreased, which increased the tension of the bonds in the structure and weakened the energy of the C–C

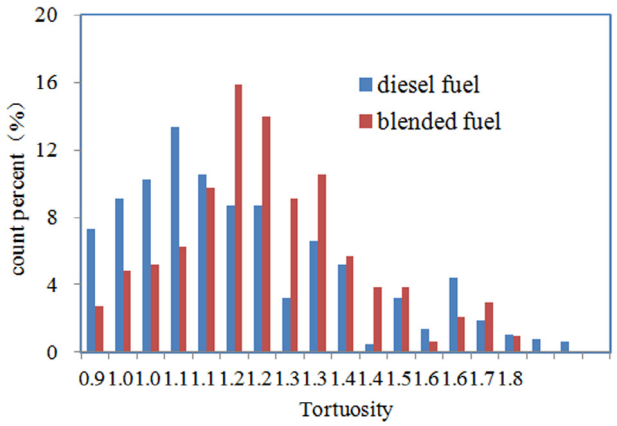

Fig. 8. Tortuosity of the particulate matter from the two test fuels.

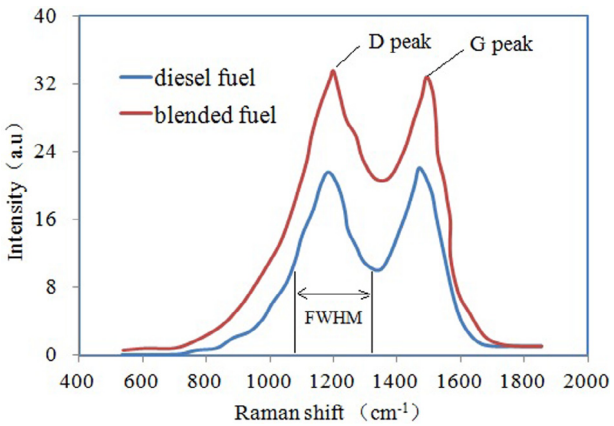

Fig. 9. The Raman spectra of the DEPM.

double bond at the bend. Structurally, the position of a single carbon atom was more convex, so the curved carbon layer was more likely to be oxidized.

Fig. 8 is the calculation result of the tortuosity of the basic carbon particles calculated from the TEM image. The tortuosity of the basic carbon particles of pure diesel combustion particles is mainly concentrated in the range of 0.9 ∼ 1.2, while that of the blended fuel combustion particles is mainly concentrated in the range of 1.1 ∼ 1.3. From this perspective, the combustion particles of the blended fuel have a stronger oxidation activity and are easier to oxidize and decompose. However, this is not consistent with the analysis results from the two parameters of the microcrystalline size and interlayer spacing. The author further calculated the mean tortuosity value of the basic carbon particles of the two fuels and found that the mean tortuosity value of the combustion particles of pure diesel fuel was 6.0, and the mean tortuosity value of the combustion particles of the blended fuel was 6.1; that is to say, the combustion of the lubricating oil did not have a special impact on the tortuosity of the basic carbon particles.

3.3.5. Degree of graphitization

The C in the DEPM is between orderly graphite and amorphous carbon. Raman spectroscopy can be used to rapidly and effectively qualitatively or quantitatively analyze the degree of graphitization of the DEPM (Gao et al., 2016; Du et al., 2017; Zhang et al., 2016, 2018). In addition, Raman spectroscopic analysis is repeatable. Three measurements were carried out on the different positions of the same sample during the Raman spectroscopy test. The peaks of the spectra obtained by the repeated tests were basically the same, indicating that the samples collected were uniform. On this basis, the Raman spectra of the particles are fitted to the Raman spectra because the first-order Raman shift range of the diesel particulate matter is 800 cm^{-1}-2000 cm^{-1}, the second-order Raman shift range is 2700 cm^{-1}-3500 cm^{-1}, and there is a frequency-doubling relationship between the Raman spectrum and the first-order Raman spectrum. Therefore, we obtained only the first-order peak fitting of the Raman spectra.

Fig. 9 shows the Raman spectra of the DEPM samples collected from the exhaust of the diesel engine fueled with the two fuels. The characteristic peaks in the Raman spectra of GRAPHITE generally appear near 1190 cm^{-1} and 1480 cm^{-1}. The former peak, formed as a result of the low-frequency vibrations of the graphite crystallites, is named the D (disorder) peak; the latter peak, formed as a result of the stretching vibrations of the C–C bonds within the graphite lattice plane, is named the G (graphite) peak. The D peak in the Raman spectra of the diesel fuel and blended fuel appears at 1184 cm^{-1} and 1201 cm^{-1}, respectively, and the G peak in their Raman spectra appears near 1473 cm^{-1} and 1494 cm^{-1}. The FWHM value of the blended fuel is 251 cm^{-1} and that of pure diesel fuel is 192 cm^{-1}. This is because blended fuel contained more PAH content. Moreover, the PAHs contained in this fuel included acenaphthylene, acenaphthene, fluorene, phenanthrene, anthracene, benzon [g, h, i] and benzo [g, h, i] fluoranthene, which formed a large variety of intermediate products during the combustion process. It was adsorbed by the DEPM in large quantities, and consequently, the chemical heterogeneity of the DEPM increased.

4. Conclusions

Based on the present experimental results, the following conclusions can be drawn:

(1) The long carbon chain components in the lubricating oil increases the cetane number of the mixed fuel, and the distillation characteristic temperature T90 of the mixed fuel increases due to the increase in heavy components such as polycyclic aromatic hydrocarbons. Compared with pure diesel, the peak particle concentration in the nuclear mode decreased by 46.5%, but the peak particle concentration in the accumulated mode increased by 47.4%.

(2) The oxygen content of the lubricating oil is higher, and the C and H have more opportunity to participate in the combustion process and oxygen reaction, prompting the particles to crack into smaller particles, leading to a decrease in the particulate matter spacing so that the particulate matter is not easily oxidized. After the combustion of the lubricating oil, due to the collision and coagulation of the ash content of the lubricating oil, the microcrystalline length of the carbon smoke particles increases, the degree of the carbon layer structure is improved, and the particles are not easily oxidized and decomposed.

(3) The combustion of the lubricating oil did not have a special impact on the tortuosity of the basic carbon particles. The PAHs contained in this fuel included acenaphthylene, acenaphthene, fluorene, phenanthrene, anthracene, benzon [g, h, i] and benzo [g, h, i] fluoranthene, which formed a wide variety of intermediate products during the combustion process. The PAHs were adsorbed by the DEPM in large quantities, and consequently, the chemical heterogeneity of the DEPM increased.

Declaration of competing interest

The authors declare that they have no known competing financial interests or personal relationships that could have appeared to influence the work reported in this paper.

Acknowledgments

The authors gratefully acknowledge the financial support from the National Natural Science Foundation of China (NSFC. 51506011, 11802039), the Natural Science Foundation of Jiangsu Province (BK20160406).

References

Bott, R.C., Kirk, K.M., Logan, M.B., et al., 2017. Diesel particulate matter and polycyclic aromatic hydrocarbons in fire stations. Environ. Sci. Process Impacts 19 (10), 1320–1326.

Dong, L., Han, W., Liang, X., et al., 2015. Comparative study on particles formation in a diesel engine when lubricating oil involved in fuel combustion. J. Chem. 2015, 1–7.

Du, J.Y., Zhou, R.S., Zhang, D.P., et al., 2017. Impacts of DOC on PM emission from diesel engine fueled with biodiesel blends. Zhongguo Huanjing Kexue/China Environ. Sci. 37 (2), 497–502.

Gao, J., Ma, C., Xia, F., et al., 2016. Raman characteristics of PM emitted by a diesel engine equipped with a NTP reactor. Fuel 185, 289–297.

Hays, M.D., Vander Wal, R.L., 2007. Heterogeneous soot nanostructure in atmospheric and combustion source aerosols. Energy Fuels 21 (2), 801–811.

Hou, B., Ren, B., Deng, R., et al., 2017. Three-dimensional electro-Fenton oxidation of N-heterocyclic compounds with a novel catalytic particle electrode: high activity, wide pH range and catalytic mechanism. Rsc Adv. 7 (25), 15455–15462.

Jiao, P., Li, Z., Shen, B., et al., 2017. Research of DPF regeneration with NOx-PM coupled chemical reaction. Appl. Therm. Eng. 110, 737–745.

Jin, H.F., Cuoci, A., Frassoldati, A., Faravelli, T., Wang, Y.Z., Li, Y.Y., Qi, F., 2014. Experimental and kinetic modeling study of PAH formation in methane coflow diffusion flames doped with n-butanol. Combust. Flame 161, 65–70.

Lin, B.Y., Gu, H., Ni, H., Guan, B., Li, Z.Z., Han, D., Gu, C., Shao, C., Huang, Z., Lin, H., 2018. Effect ofmixing methane, ethane, propane and ethylene on the soot particle sizedistribution in a premixed propene flame. Combust. Flame 193, 54–60.

Lin, S.L., Tsai, J.H., Chen, S.J., et al., 2017. Emissions of polycyclic aromatic hydrocarbons and particle-bound metals from a diesel engine generator fueled with waste cooking oil-based biodiesel blends. Aerosol Air Qual. Res. 17 (6), 1579–1589.

Llamas, A., Al-Lal, A.M., García-Martínez, M.J., et al., 2017. Polycyclic aromatic hydrocarbons (PAHs) produced in the combustion of fatty acid alkyl esters from different feedstocks: Quantification, statistical analysis and mechanisms of formation. Sci. Total Environ. 586, 446–456.

Martini, A., Ramasamy, U.S., Len, M., 2018. Review of viscosity modifier lubricant additives. Tribol. Lett. 66 (2), 58.

R'Mili, B., Boreave, A., Meme, A., et al., 2018. Physico-chemical characterization of fine and ultrafine particles emitted during DPF active regeneration of Euro5 Diesel vehicles. Environ. Sci. Technol. 52 (5), 3312–3319.

Serrano, J.R., Bermúdez, V., Piqueras, P., et al., 2017. On the impact of DPF down-sizing and cellular geometry on filtration efficiency in pre- and post-turbine placement. J. Aerosol Sci. 113, 20–35.

Sonntag, D.B., Bailey, C.R., Fulper, C.R., et al., 2012. Contribution of lubricating oil to particulate matter emissions from light-duty gasoline vehicles in Kansas City. Environ. Sci. Technol. 46 (7), 4191–4199.

Tan, P.Q., Li, Y., Shen, H.Y., 2018. Exhaust particle properties from a light duty diesel engine using different ash content lubricating oil. J. Energy Inst. 91 (1), 55–64.

Tan, P.Q., Wang, D.Y., 2017. Effects of sulfur content and ash content in lubricating oil on the aggregate morphology and nanostructure of diesel particulate matter. Energy Fuels 32 (1), 713–724.

Wang, H., 2011. Formation of nascent soot and other condensed-phase materials inflames. Proc. Combust. Inst. 33, 41–67.

Wei, L.J., Cheung, C.S., Huang, Z.H., 2014a. Effect of n-pentanol addition on the combustion, performance and emission characteristics of a direct-injection diesel engine. Energy 70, 72–80.

Wei, Y., Wang, K., Wang, W., et al., 2014b. Comparison study on the emission characteristics of diesel- and dimethyl ether-originated particulate matters. Appl. Energy 130 (5), 357–369.

Worton, D.R., Isaacman, G., Gentner, D.R., et al., 2014. Lubricating oil dominates primary organic aerosol emissions from motor vehicles. Environ. Sci. Technol. 48 (7), 3698–3706.

Yehliu, K., Wal, R.L.V., Boehman, André L., 2011a. A comparison of soot nanostructure obtained using two high resolution transmission electron microscopy image analysis algorithms. Carbon 49 (13), 4256–4268.

Yehliu, K., Wal, R.L.V., Boehman, André L., 2011b. Development of an HRTEM image analysis method to quantify carbon nanostructure. Combust. Flame 158 (9), 1837–1851.

Zhang, Y., Tao, W., Li, Z., et al., 2018. Experimental studies on the combustion and particulate matter emission characteristics of biodiesel surrogate component/diesel. Appl. Therm. Eng. 131, 565–575.

Zhang, C., Wang, T., Ding, Y., 2017. Influence of Pt particle size on the activity of Pt/AC catalyst in selective oxidation of glycerol to lactic acid. Catal. Lett. 147 (5), 1–7.

Zhang, Jian, Wang, Zhong, Qu, Lei, et al., 2016. The analysis of Raman spectra of particulate matters emitted from biodiesel-diesel blend fuels. Spectrosc. Spectr. Anal. 36 (8), 2505–2509.